Supplemental Figures

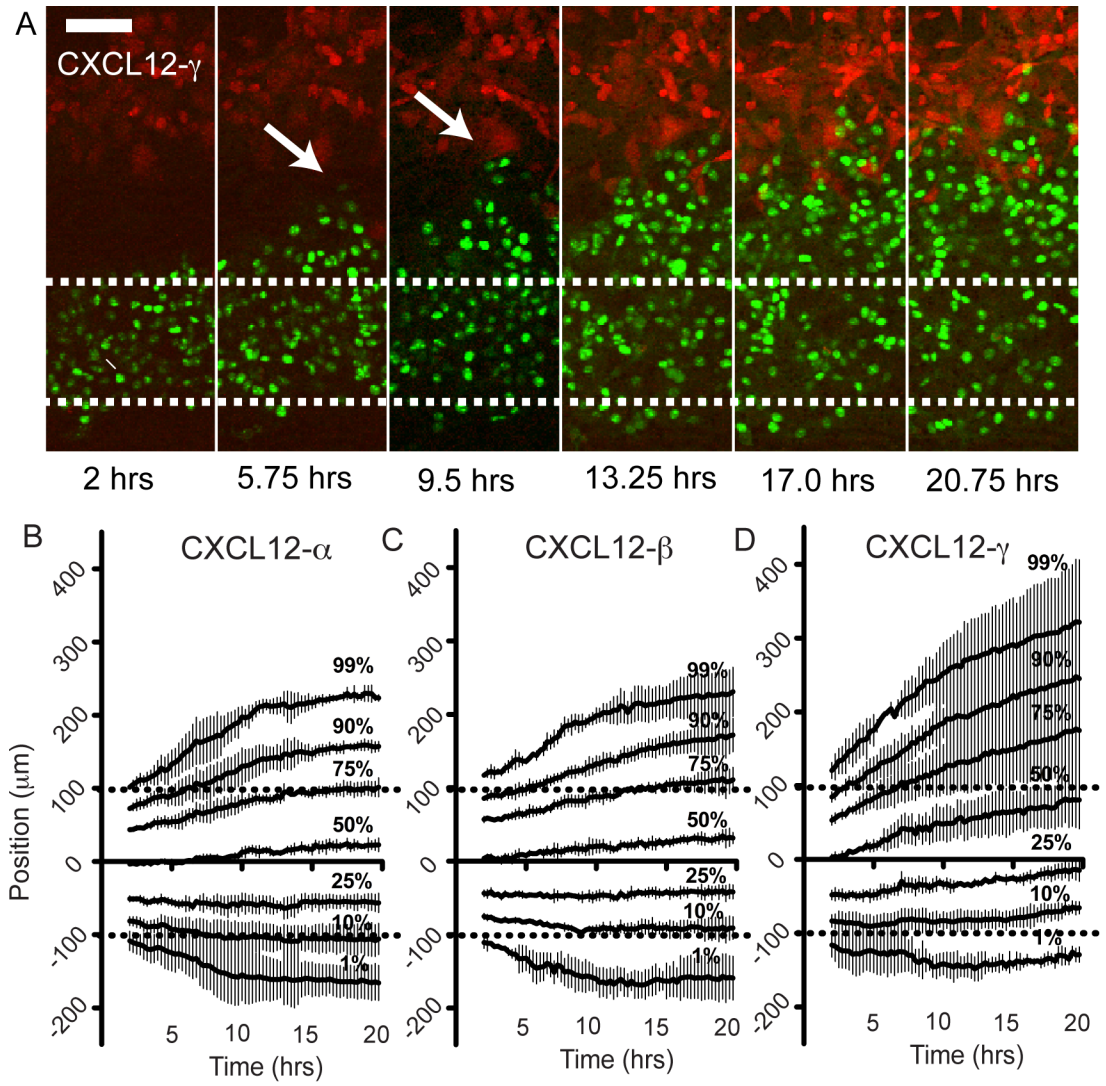

Figure S1. CXCL12-γ enhances initial chemotaxis of CXCR4+ cells. *(A)* Time lapse images of CXCR4+ cells (green) migrating towards CXCL12-γ secreting cells (red). Imaging began two hours after final seeding (t=2 hrs), followed by images every 15 minutes for ~20 hours. Representative images are shown. The dotted white lines designate the channel location and starting position. The arrows denote leading sprout formation and the scale bar indicates 100 μm length. Representative time lapse videos are found in Supplemental Video V1. *(B-D)* Chemotaxis of CXCR4+ cells toward cells secreting various CXCL12 isoforms was quantified by live cell microscopy. Data show percentile distributions of CXCR4+ cell positions over time ± S.D. beginning two hours after patterning cells (n = 3 individual set ups, ~1200 cells total). The 50% line is the median position of the cells. The dashed lines denote the channel boundries where cells were initially patterned.

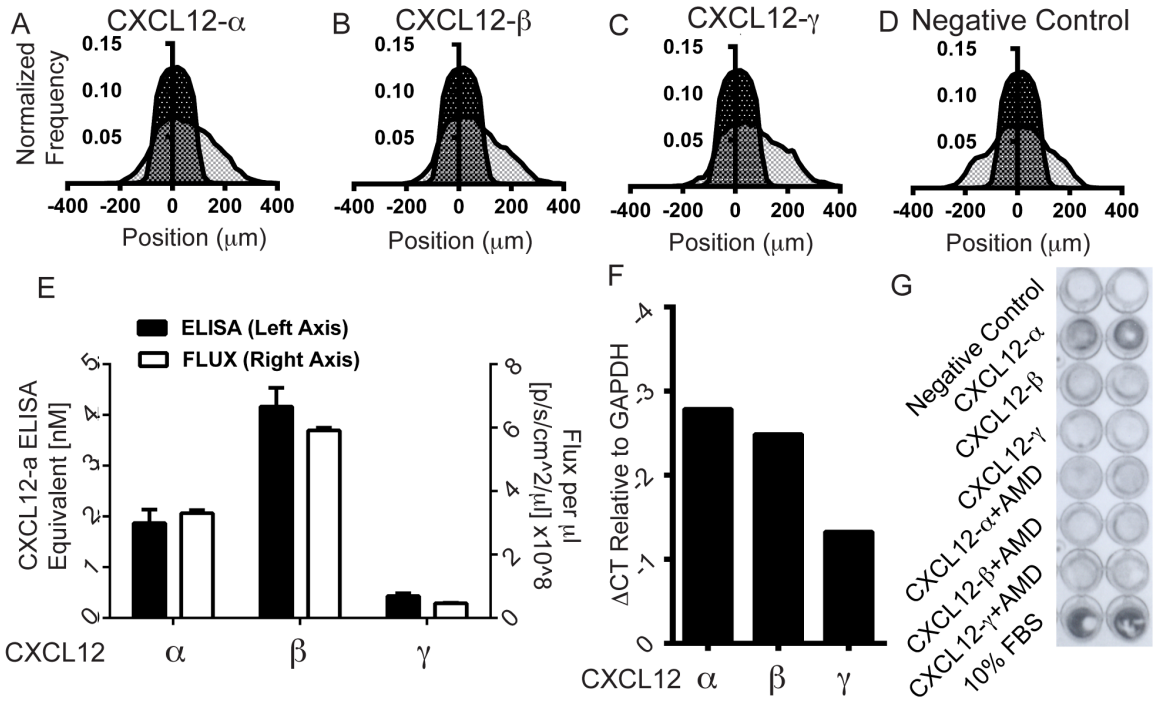

Figure S2. Increased chemotaxis of CXCR4+ cells toward CXCL12-γ. *(A-D)* Position frequency distribution of CXCR4+ cells relative to the starting point (channel boundaries). Frequencies are normalized to the number of cells per view. These data are composite distributions for each CXCL12-isoform representing 10-11 devices with 6 view fields each (~15x10^3 cells total per histogram). The black distribution represents the pooled initial distribution. Graphs depict chemotaxis toward CXCL12 as a shift to positive positions with higher values denoting greater distances traveled by cells. *(E)* Production of CXCL12 isoforms after 24 hours based on corresponding *Gaussia* luciferase activity and CXCL12-α ELISA equivalent measurements. We measured CXCL12-isoform content in supernatants from 10^6 231 cells secreting individual CXCL12-isoforms. We measured *Gaussia* luciferase activity with 1:5 final dilution of supernatants in a 1:100 dilution in PBS of 1 mg per ml coelenterazine (50 μl total). Data are reported as mean ± S.E.M. for 6 measurements each in two independent setups with paired ELISA and bioluminescence measurements (n = 12 total). Each ELISA well was measured in quadruplicate. *(F)* Relative qRT-PCR amplification cycle number (ΔCT) as compared to GAPDH. We measured comparable mRNA levels of CXCL12-isoforms in our transduced cells. CXCL12 was not detectable in the parental cells. *(G)* Transwell migration towards 100 ng/ml CXCL12-isoforms in the absence or presence of CXCR4 inhibitor AMD3100 (1 μM). Cells migrating through the membrane in response to equal amounts of cell-secreted CXCL12 isoforms based on *Gaussia* luciferase activity were detected by staining with crystal violet. Darker staining shows relatively greater cell migration. 10% fetal bovine serum (FBS) was used as a positive control.

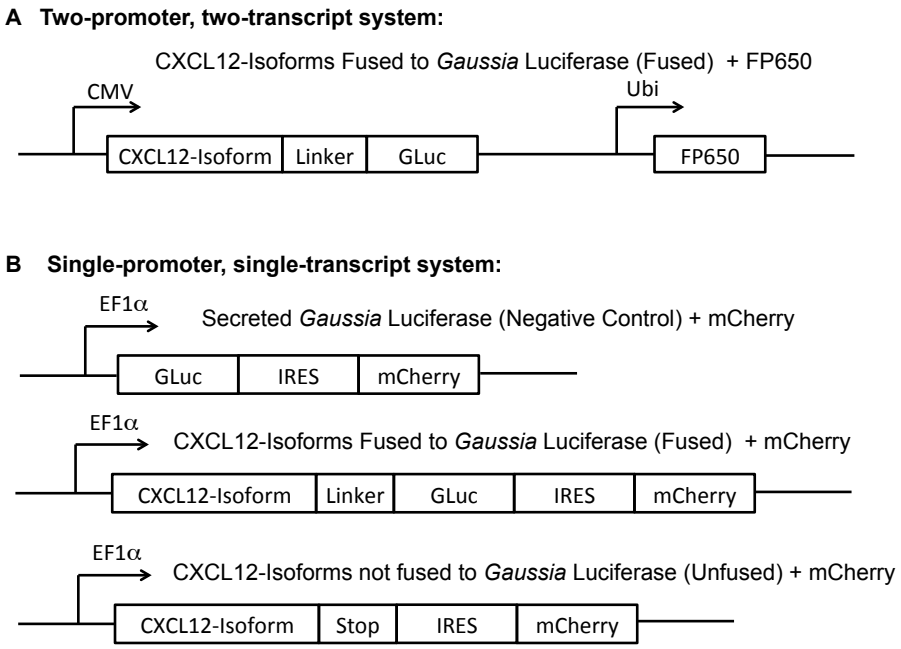

Figure S3. CXCL12-isoform vector construction. We used two viral constructs to express CXCL12-isoforms in mammalian cells. *(A)* Schematic representation of the two-part construct with CXCL12-isoforms fused to *Gaussia* luciferase under one the CMV promoter and the far-red fluorescent protein under the Ubi promoter. This strategy forgoes the ability to express and sort for *Gaussia* luciferase-unfused CXCL12. We used this construction for most data represented in this paper. *(B)* Schematic representations of the one-transcript expression system using and internal ribosomal entry site (IRES) separating two genes of interest under a single EF1α promoter. This strategy enabled more quantitative control of CXCL12 abundance based on proportional expression with mCherry. The IRES construct also enabled flow cytometry sorting for CXCL12 with a stop codon rather than linked to *Gaussia* luciferase. We used the IRES construct for comparison of the biological effect of recombinant *Gaussia* luciferase fusions in Figure S2.

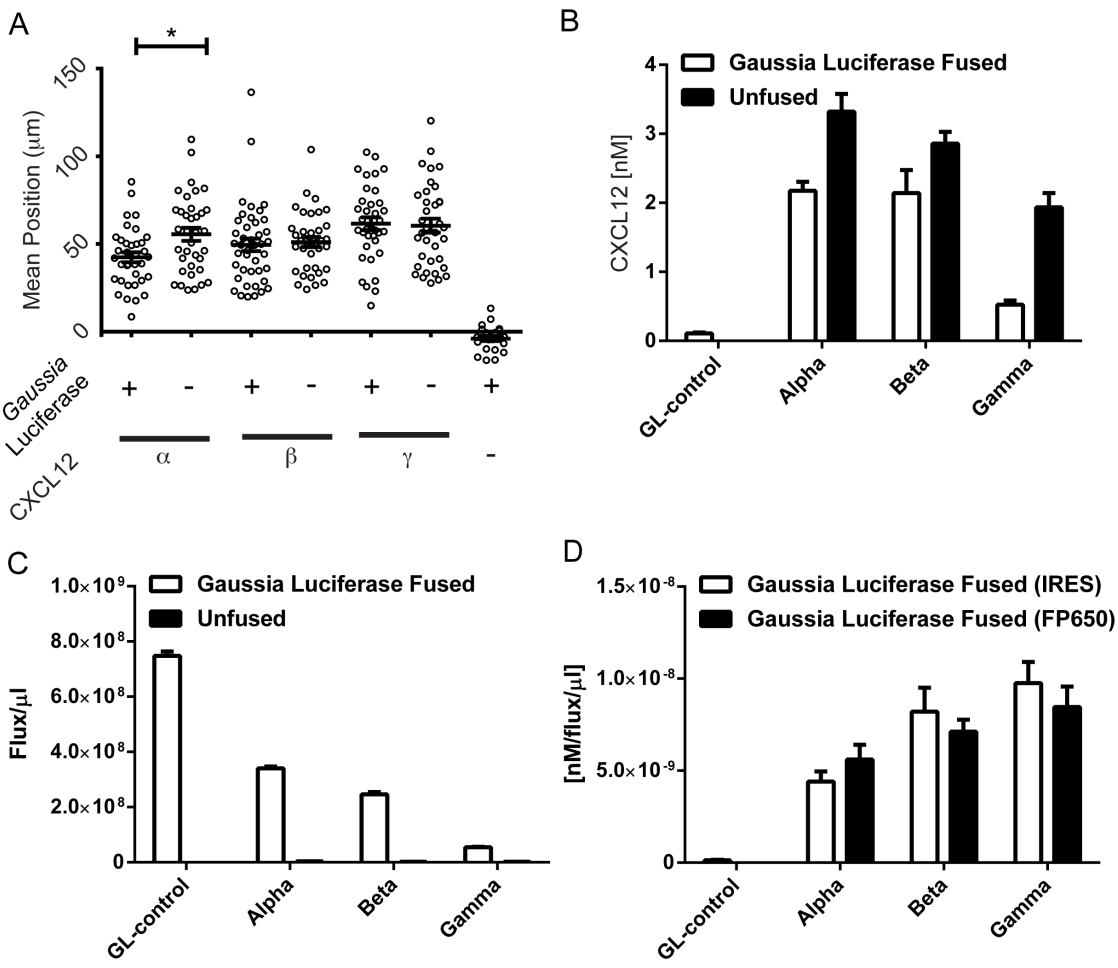

Figure S4. Characterization to recombinant CXCL12-isoforms with and without *Gaussia* luciferase fusions. *(A)* Average position of CXCR4+ cells after 24 hours of migration toward cells expressing IRES constructs for CXCL12-α, β, or γ with (+) and without (-) recombinant *Gaussia* luciferase fusion, as described in Figure S2 part B. The negative control cells secrete *Gaussia* luciferase without CXCL12. Data are shown as mean values ± S.E.M. (n=6 view fields for 4-6 devices per condition, similar to described in Fig. 1). The bars represent the statistical comparison of all fractions to the non-secreting control (0%). Statistical demarcations directly above data are comparisons to the 100% secreting fraction (* $p<0.005$). Matched conditions were performed in parallel. We measured secretion of IRES CXCL12 constructs based on corresponding equivalent ELISA reactivity, which was developed and calibrated towards CXCL12-α *(B)* and *Gaussia* luciferase activity *(C)* in the supernatants from 10^6 231 cells in 30 mm dishes after 24 hours. *(B)* By ELISA measurements, CXCL12 expressed without *Gaussa* luciferase fusion was more abundant and/or more efficiently measured by ELISA. *(C)* Corresponding bioluminescent imaging of *Gaussia* luciferase activity revealed only background signal from the unfused CXCL12 constructs but substantial signal from the negative control secreted *Gaussia* luciferase (GL-control) and from the CXCL12-fusions. Bioluminescence

data is normalized per µl of supernatant added. *(D)* Comparison of the measured ELISA readings per bioluminescent flux revealed a rank-order increase in the nM per flux per µl quantitation of CXCL12-fusions from both the IRES constructs and the FP650 constructs. These measures were on the same order of magnitude for all three isoforms, allowing us to use *Gaussia* luciferase activity to estimate the quantity of CXCL12-isoforms in supernatants. Data are reported as mean ± S.E.M. for 6 measurements each in two independent setups with paired ELISA and bioluminescence measurements (n = 12 total). Each ELISA well was measured in quadruplicate.

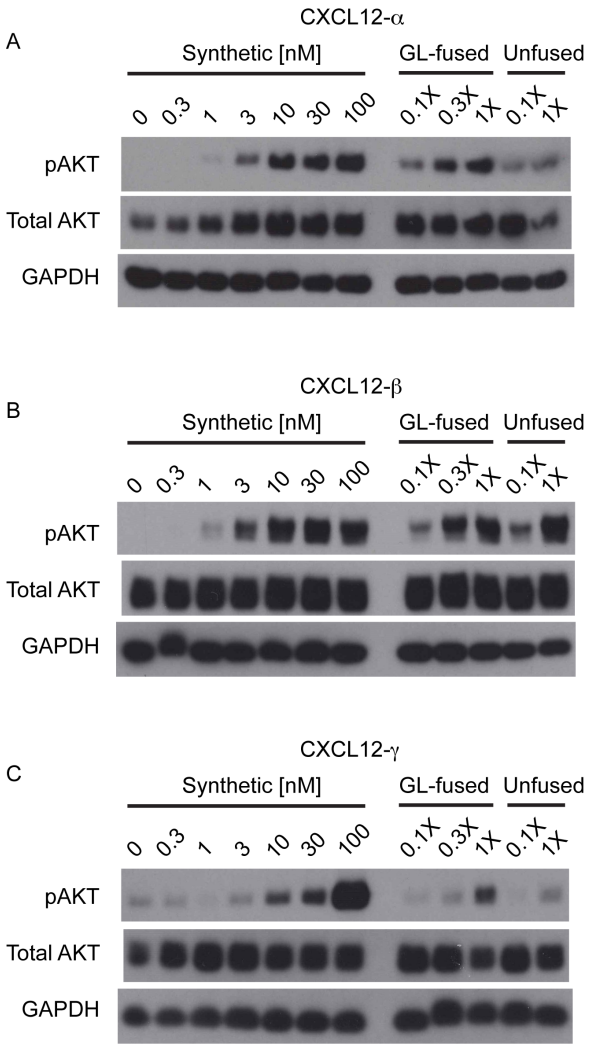

Figure S5. CXCL12-isoform induction of AKT phosphorylation. *(A-C)* Western blot analysis of AKT phosphorylation downstream of CXCR4 in MDA-MB-231 cells for CXCL12-α, -β, and -γ, respectively. We measured total AKT and GAPDH as loading controls.

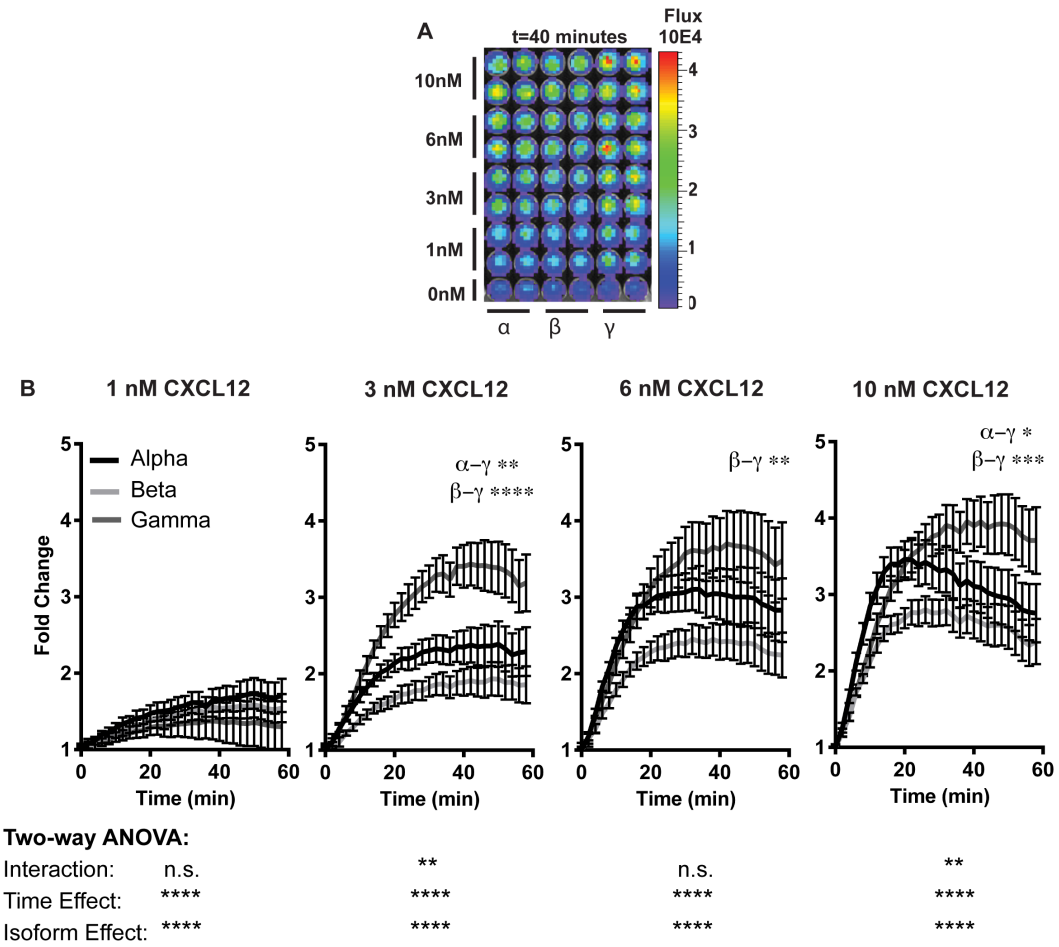

Figure S6. Representative bioluminescence images of β-arrestin 2 recruitment to CXCR4 in response to CXCL12 isoforms. Dilutions of equimolar concentrations of recombinant CXCL12 isoforms were applied simultaneously to cells. This image was taken at t=40 minutes of a 1 hour time course. Scale bar depicts range of photon flux (p/s/cm^2) values with the pseudocolor dislay scale showing red and blue as highest and lowest values, respectively. The image depicted is representative two experimental runs.

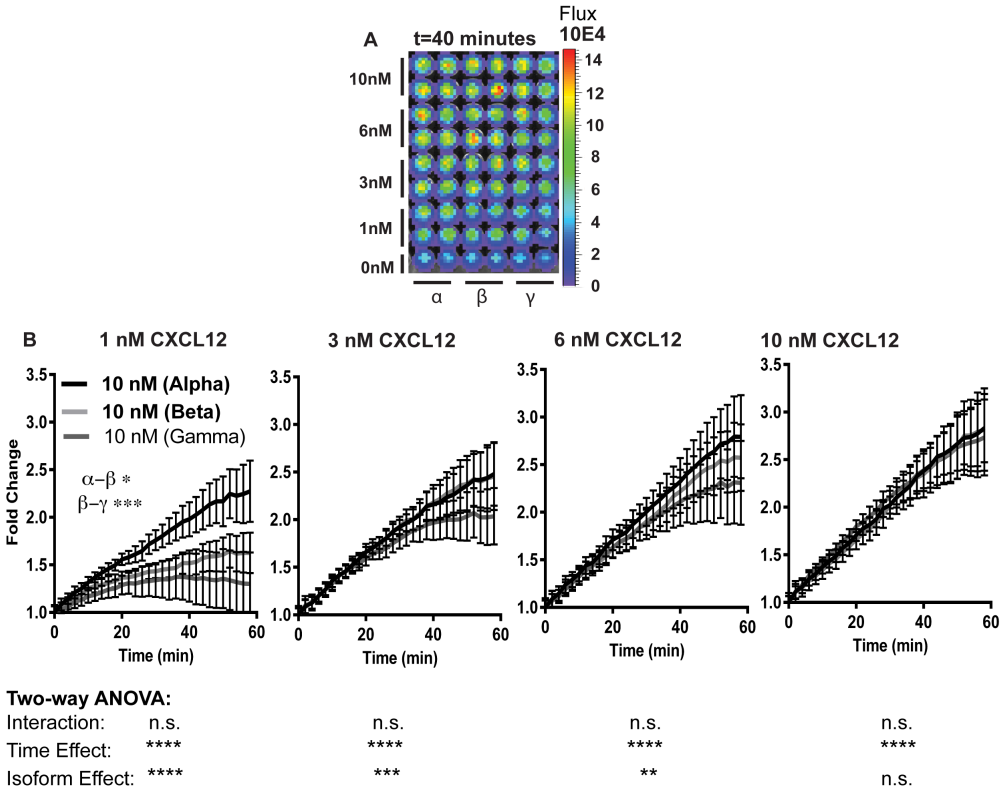

Figure S7. Representative bioluminescence images of β-arrestin 2 recruitment to CXCR7 in response to CXCL12 isoforms. Cells expressing a luciferase complementation reporter for association of CXCR7 and β-arrestin 2 were incubated with increasing equimolar concentrations of synthetic CXCL12-α, β, or γ. Representative bioluminescence image from t=40 minutes from a one hour time course. Scale bar depicts range of photon flux (p/s/cm^2) values with pseudocolor display. The image depicted is representative two experimental runs.

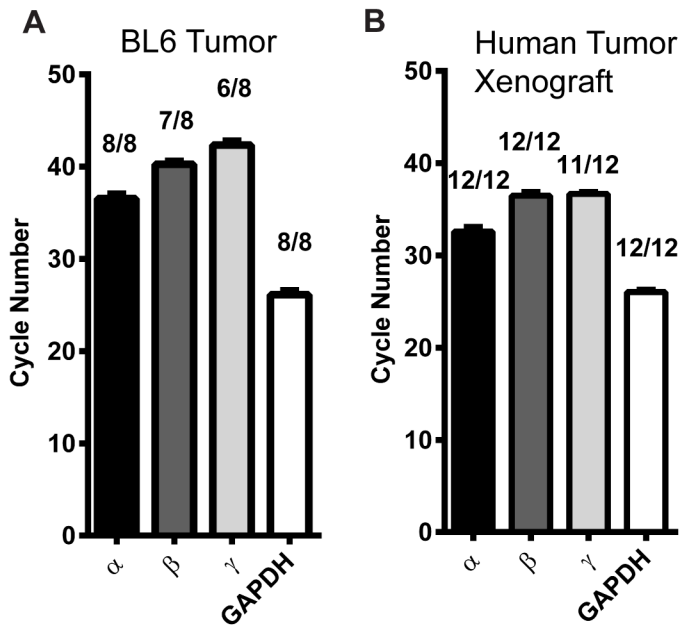

Figure S8. Mouse expression of CXCL12-isoforms in primary breast tumors. Quantitative RT-PCR cycle numbers are reported for orthotopic implants of *(A)* syngenic implants of E0771 breast cancer cells in C57BL/6mice and *(D)* human xenograft of MDA-MB-231 cells in NSG mice. Tissues homogenates were analyzed from primary tumors. Numerals above data represent the fraction of samples positive for each transcript. Transcripts amplified below 40 qRT-PCR cycles we denoted as positive. Amplified gene product purity was also confirmed via gel electrophoresis.

Supplemental Results

Characterization of secreted *Gaussia* luciferase CXCL12-isoform-fusions

The single promoter, IRES-linked CXCL12 and mCherry construct facilitates characterization of CXCL12-isoforms fused or not fused with *Gaussia* luciferase. The internal ribosomal entry site (IRES)-linkage promotes proportional expression of both proteins, but limits translational efficiency and total protein levels as compared to single protein transcripts. For this reason, we also developed a vector to co-express CXCL12-isoforms fused to *Gaussia* luciferase and a far-red fluorescent protein (FP650) from two different promoters.

We used the IRES system to evaluate effects of the *Gaussia* luciferase fusion on biological activity of CXCL12-isoforms (Fig. S4). To characterize levels of secreted CXCL12 *Gaussia* luciferase fusions, we complemented ELISA reactivity with bioluminescence imaging. Although polyclonal ELISA antibodies were developed towards CXCL12-α, we measured the relative ELISA ng per bioluminescence flux to be on the same order of magnitude for all isoforms. All CXCL12-isoforms elicited chemotaxis of CXCR4+ cells independent of fusion to *Gaussia* luciferase. To measure the biological effect of recombinant *Gaussia* luciferase fusions, we measured phosphorylation of AKT, a known downstream target of CXCL12-CXCR4 signaling (Fig. S5). As compared with recombinant CXCL12-isoforms, CXCL12 secreted by 231 cells stimulated levels of AKT phosphorylation corresponding to the measured ELISA-based concentrations for each isoform, independent of fusion to *Gaussia* luciferase. For the *Gaussia* luciferase fusions, our bioluminescence-based measurement of chemokine concentration corresponded with the Western blot phosphorylation of AKT as compared with recombinant CXCL12-isoforms. In combination with our prior studies of CXCL12-α, these data show that CXCL12 isoforms retain expected biological activity when fused to *Gaussia* luciferase (Fig. S4-5)[32].

Since IRES-linkage may limit translational efficiency of both products, we used a two-promoter system to express higher levels of CXCL12-isoform fusions with *Gaussia* luciferase for subsequent studies (Fig. S2A). Similar to the IRES-linked expression system, ELISA and bioluminescence imaging provided complementary measures of chemokine production (Fig. 2F and S2B-D). We sorted cells for equal expression of co-expressed FP650 fluorescent protein, yielding comparable levels of mRNA for CXCL12 α and β with slightly lower levels of CXCL12-γ (Fig 2G). We note that CXCL12 transcripts were undetectable in parental 231 cells, so source cells secreted only the desired isoform (data not shown).

Supplemental Discussion

For the simplest semi-quantitative conceptualization of increased CXCL12-γ potency, we posit that CXCL12 is a bivalent ligand between CXCR4 and heparan sulfate, a major component of cell surfaces and the extracellular compartment. Previous studies have shown that co-localization of heparan sulfate with CXCR4 cooperatively increases local concentrations of CXCL12, thus promoting signaling[1]. To estimate the overall affinity of CXCL12-isoforms to CXCR4 and heparan sulfate, we extend a model developed to calculate the bivalent affinity of polymer-linked ligands[2,3]. The bivalent affinity is a multiplicative function of the two monovalent affinities of CXCL12 for CXCR4 and heparan sulfate (K_{R4} and K_{HS}) with the effective concentration of the multiple-binding ligand (C_{Eff}). The parameter C_{Eff} is based on molecular size, shape, and rigidity of the multiple-binding ligand, which we assume to be the same between CXCL12 isoforms and therefore we leave this as a constant. We also assume the distance between heparan sulfates and CXCR4 not to be limiting based on the high abundance and flexibility of heparan sulfates[4]. Multiplication of the binding constant for CXCL12-isoforms to CXCR4 or heparan sulfate reveals ~6 fold greater apparent affinity for CXCL12-γ as compared to the α-isoform (Table S1). Although only semi-quantitative, this conceptual framework provides a potential mechanism for increased chemotactic potency of CXCL12-γ.

Table S2. Affinities for CXCL12 isoforms towards CXCR4, heparan sulfate, and divalent CXCR4-HS complex.

	CXCL12-Isoforms		
Tumor Grade:	α	β	γ
CXCR4 (IC50 ~ K_{R4})[5]	15 nM	--	350 nM
Heparan Sulfate (K_{HS})[6]	200 nM	53 nM	1.5 nM
C_{Eff}*K_{R4}*K_{HS}	C_{Eff}*3000	--	C_{Eff}*525

Note: IC_{50} is proportional between α and γ for CXCR4 so we use it as a surrogate for K_d for CXCL12-γ. We assume C_{Eff} to be equal for both isoforms based on structural similarities.

1 Valenzuela-Fernandez, A. *et al.* Optimal inhibition of X4 HIV isolates by the CXC chemokine stromal cell-derived factor 1 alpha requires interaction with cell surface heparan sulfate proteoglycans. *J Biol Chem.* **276**, 26550-26558. Epub 22001 May 26514. (2001).

2 Kane, R. S. Thermodynamics of Multivalent Interactions: Influence of the Linker. *Langmuir* **26**, 8636-8640, doi:10.1021/la9047193 (2010).

3 Krishnamurthy, V. M., Semetey, V., Bracher, P. J., Shen, N. & Whitesides, G. M. Dependence of effective molarity on linker length for an intramolecular protein-ligand system. *J Am Chem Soc.* **129**, 1312-1320. (2007).

4 Kramer, R. H. & Karpen, J. W. Spanning binding sites on allosteric proteins with polymer-linked ligand dimers. *Nature.* **395**, 710-713. (1998).

5 Laguri, C. *et al.* The novel CXCL12gamma isoform encodes an unstructured cationic domain which regulates bioactivity and interaction with both glycosaminoglycans and CXCR4. *PLoS One* **2**, e1110 (2007).

6 Rueda, P. *et al.* The CXCL12gamma chemokine displays unprecedented structural and functional properties that make it a paradigm of chemoattractant proteins. *PLoS One* **3**, e2543 (2008).

Supplemental Methods

Text S1. ImageJ Script for Cell Position. The following imageJ script takes corresponding 8-bit phase contrast and fluorescent images and maps the coordinate of every cell. The script converts fluorescent images to binary images for a range of threshold values to identify both bright and dim cells. The threshold scan also identifies duplicate counts, which we exclude using an embedded loop comparison. The output coordinates were analyzed in Microsoft Excel.

```
macro "automated migration" {
waitForUser("Open Phase Contrast and Draw Rectangle");
run("Set Measurements...", "area center limit redirect=None decimal=3");
run("Clear Results");
myImageID = getImageID(); //get Image information

//Make Rectangle Manually, Delay, Check the Channel Position
setTool(0);
if(selectionType() != 0)
     exit("Sorry, no rectangle");
run("Measure");
area=getResult("Area",0);
xm=getResult("XM",0);
ym=getResult("YM",0);

run("Close All");
waitForUser("Open Fluorescence IMG");
myImageID2 = getImageID();
selectImage(myImageID2);
direct = getInfo("image.directory");
filename = getInfo("image.filename");

setThreshold(20, 255);
run("Convert to Mask");
run("Open");
run("Watershed");
run("Analyze Particles...", "size=30-300 circularity=0.00-1.00 show=Ellipses display clear");

for(i=nResults; i>0; i--) {
     areai=getResult("Area",i-1);
     xmi=getResult("XM",i-1);
     ymi=getResult("YM",i-1);
     setResult("Area",i,areai);
     setResult("XM",i,xmi);

setResult("YM",i,ymi);}
```

```
setResult("Area",0,area);
setResult("XM",0,xm);
setResult("YM",0,ym);
updateResults();
run("Close All");

//Loop through thresholds, 5 threhold incraments

i=25;
while(i<75){open(direct+"/"+filename);
    setThreshold(i, 255);
    run("Convert to Mask");
    run("Open");
    run("Watershed");
        run("Analyze Particles...", "size=30-300 circularity=0.00-1.00 show=Ellipses display");
        run("Close All");
        i=i+5;}

//Loop through thresholds, 20 threshold increments

i=75;
while(i<250){open(direct+"/"+filename);
    setThreshold(i, 255);
    run("Convert to Mask");
    run("Open");
    run("Watershed");
        run("Analyze Particles...", "size=30-300 circularity=0.00-1.00 show=Ellipses display");
        run("Close All");
        i=i+20;}

//Remove Data with Duplicates,
run("Close All");

for(i=1; i<=nResults; i++) {
    for(j=i+1; j<nResults; j++)  {

//Speeds up program by not Processing NaNs as duplicates
            if(getResult("XM",j)==NaN)
                j=nResults;
            if( abs(getResult("XM",i)-getResult("XM",j)) < 5 && abs(getResult("YM",i)-
getResult("YM",j)) < 5) { for(k=j+1;k<nResults;k++){
                    areak=getResult("Area",k);
                    xmk=getResult("XM",k);
                    ymk=getResult("YM",k);
                    setResult("Area",k-1,areak);
                    setResult("XM",k-1,xmk);
                    setResult("YM",k-1,ymk);
                    setResult("Area",k,NaN);
                    setResult("XM",k,NaN);
                    setResult("YM",k,NaN);
                }}}}

setResult("Area",0,area);
setResult("XM",0,xm);
setResult("YM",0,ym);
updateResults();
```

```
//Starts over for a new image
run("automated migration");
}
```